Organic & Biomolecular Chemistry

ROYAL SOCIETY OF CHEMISTRY

PAPER

View Article Online
View Journal | View Issue



Cite this: *Org. Biomol. Chem.*, 2025, **23**, 4240

# Photoswitchable agonists for visible-light activation of the Wnt signaling pathway†

Shifa Ahmad,[a,b] P. K. Hashim,[a,b] Masamichi Imajo,[c] Nusaiba Madappuram Cheruthu,[a,b] Kiyonori Takahashi,[a,d] Shinya Tanaka,[c,e] Takayoshi Nakamura[a,d] and Nobuyuki Tamaoki *[a,b]

Based on the known Wnt agonist **BML-284**, we designed and synthesized photoswitchable azo derivative compounds that can act as agonists for the Wnt signaling pathway. These photoswitchable agonists were shown to undergo reversible *trans–cis* isomerization upon being irradiated with visible light, but only the *cis* isomer was observed to activate the Wnt signaling pathway, using a luminescense-based reporter assay in cultured cells. One of the compounds, denoted as compound **2**, showed ~88% agonist activity after being subjected to visible light irradiation in comparison to the non-photoswitchable **BML-284**. We also were able to selectively activate the Wnt signaling pathway using **2** and light irradiation at a specific region of interest in a model cell culture system, highlighting the ability to achieve spatiotemporal regulation.

Received 13th November 2024,
Accepted 31st March 2025

DOI: 10.1039/d4ob01827c

rsc.li/obc



## Introduction

Wnt signaling plays an important role in many biological processes, such as gene regulation, embryonic development, and the progression of cancer.[1–3] Its impact on these fundamental processes makes it a key target for research and potential therapeutic applications.[4,5] It is also an essential pathway for cell adhesion, proliferation and differentiation.[6] The downstream signal transduction in the Wnt signaling pathway is initiated by the binding of Wnt ligand protein to its receptor (Frizzled) on the cell membrane. A key effector protein of Wnt signaling pathway is β-catenin. In cells, β-catenin is degraded by the axin-APC (adenomatous polyposis coli)-GSK-3β (glycogen synthase kinase 3β) complex. The Wnt ligand binding inhibits the function of the axin-APC-GSK-3β complex, causing the accumulation of β-catenin in the cell cytoplasm. The β-catenin subsequently translocates to the nucleus and forms a complex with T-cell factor/lymphoid-enhancer factor (TCF/LEF), thereby regulating the transcription of target genes. Small-molecule agonists or antagonists can also activate or inhibit the Wnt signaling pathway.[7,8] For instance, **BML-284** is a cell-permeable Wnt signaling agonist shown to function both in cell culture and *Xenopus* models.[7]

In signal transduction, downstream responses often depend on the precise location and duration of protein phosphorylation. Particularly, the Wnt pathway has been shown to be a major morphogenetic switch in stem cell differentiation, and its spatial localization is critical.[6,9] Optical control of signal transduction is one way to achieve high spatiotemporal resolution. We envisioned developing a small-molecule-based photoswitchable agonist for optically controlling the Wnt signaling pathway. Optogenetical control of the Wnt signaling pathway that involves light-inducible protein–protein interactions has been reported.[10,11] However, controlling the Wnt signalling pathway *via* an optogenetic approach can be more complicated than a small-molecule-based approach, which does not require genetic modification.

In the field of photopharmacology, molecular photoswitches are incorporated into the biologically active small molecules to control their activity in a specific location and at a specific time.[12] Molecular photoswitches show reversible structural changes between two forms when exposed to light, affecting their effectiveness against biological targets. Although many different types of photoswitches including dithienylethenes[13–15] are known, the most common types of photoswitches used for photopharmacology are those based on azobenzenes.

[a]*Research Institute for Electronic Science, Hokkaido University, Kita20, Nishi 10, Kita-ku, Sapporo, Hokkaido, 001-0020, Japan. E-mail: tamaoki@es.hokudai.ac.jp*
[b]*Graduate School of Life Science, Hokkaido University, Kita 10, Nishi 8, Kita-ku, Sapporo, Hokkaido, 060-0810, Japan*
[c]*Institute for Chemical Reaction Design and Discovery (WPI-ICReDD), Hokkaido University, N21, W10, Kita-ku, Sapporo 001-0021, Japan*
[d]*Graduate School of Environmental Science, Hokkaido University, Sapporo, Hokkaido 060-0810, Japan*
[e]*Department of Cancer Pathology, Faculty of Medicine, Hokkaido University, N15, W7, Kita-ku, Sapporo 060-8638, Japan*

† Electronic supplementary information (ESI) available. CCDC 2389889 2389890. For ESI and crystallographic data in CIF or other electronic format see DOI: https://doi.org/10.1039/d4ob01827c

Our group and others have achieved photocontrol over various biological systems by incorporating azobenzene-based photoswitches into biologically active small molecules.[16–18] For instance, photoswitchable substrates and inhibitors of ion channels,[19] G-protein coupled receptors,[20] motor proteins,[21,22] kinases,[23] proteases[24] and cellular signaling pathways[25,26] have been developed. In our current study, we developed compounds **1** and **2**, shown to be photoswitchable azo derivatives of the Wnt signaling agonist **BML-284**. The biologically active form of **BML-284** was found to be a bent structure with the 1,2-methylenedioxybenzene motif nearly perpendicular to the plane of aminopyrimidine motif in the host protein T2R-TTL (Protein Data Bank (PDB: 7CEK)) (Fig. 1 and S29†). Due to this bent structure expected only in the respective *cis* forms of compounds **1** and **2**, these *cis* forms and not the *trans* ones were considered to likely be active as Wnt agonists. Our results showed *cis*-**2** functioning as a relatively good agonist for the Wnt signaling pathway. We also demonstrated selective activation of the Wnt signaling pathway with a spatial resolution of 10 mm upon light irradiation of **2** in a model cell culture system.

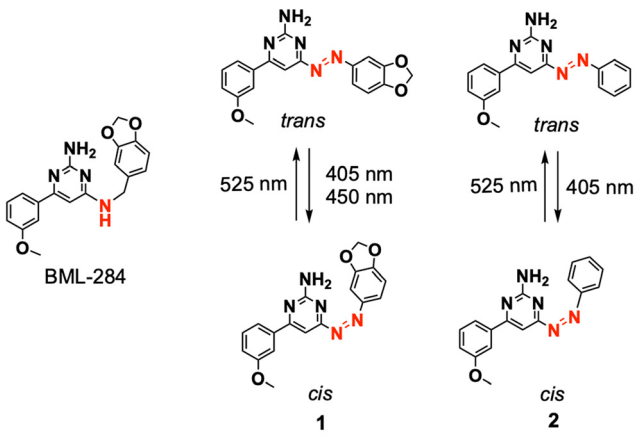


**Fig. 1** Molecular structures of a non-photoswitchable Wnt agonist **BML-284** and photoswitchable Wnt agonists **1** and **2** along with their reversible *trans*–*cis* isomerization activated by visible light (405 nm, 450 nm, or 525 nm).

## Results and discussion

### Synthesis and photophysical studies

Compounds **1** and **2** were synthesized by carrying out a Mills reaction between diamino methoxyphenyl pyrimidine and nitrosobenzene derivatives (Fig. 2a, Schemes S3 and S4†). The formed azo derivatives **1** and **2** were characterized using $^{1}$H NMR, $^{13}$C NMR and mass spectroscopy. To unambigurously establish the chemical structures of **1** and **2**, we determined single-crystal X-ray structures of them and found an intact amine group at position 2 of the pyrimidine ring (Fig. 2b). The photophysical properties of **1** and **2** in organic and aqueous solutions were studied using UV-Vis absorption spectroscopy. The absorption spectrum of **1** (100% *trans* isomer; confirmed using NMR Fig. S5†) without light illumination exhibited a $\pi$–$\pi^*$ transition band at 380 nm, which was red-shifted by 45 nm compared with that of azobenzene (Fig. 2c, black curve). The red-shifted absorption allowed us to use visible light for its isomerization. Upon being illuminated with 405 nm-wavelength light, it reached a photostationary state ($PSS_{405\ nm}$), where the *cis* isomer was predominantly formed

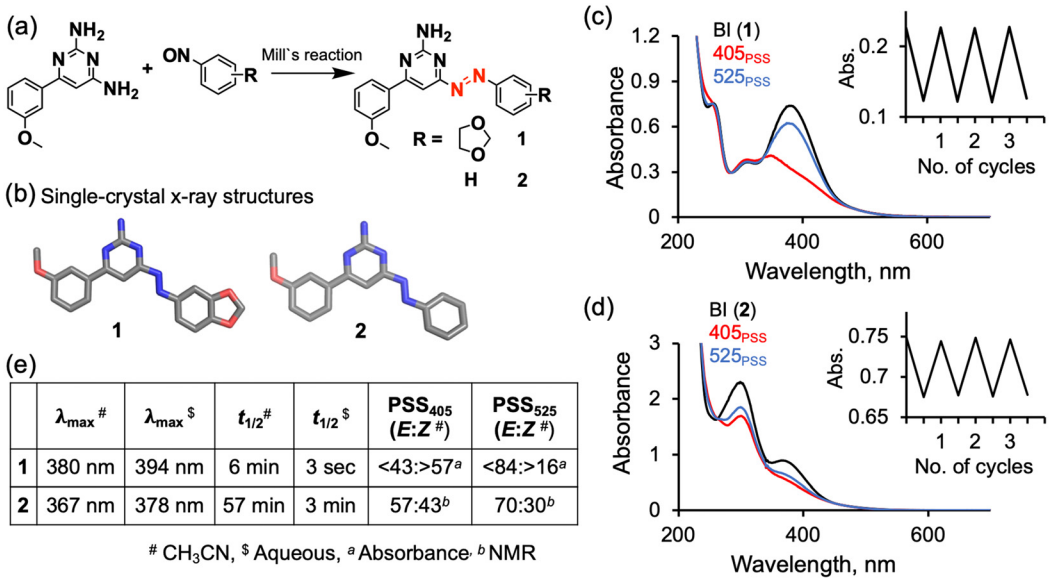


(e)

| | $\lambda_{max}$ # | $\lambda_{max}$ $ | $t_{1/2}$ # | $t_{1/2}$ $ | $PSS_{405}$ (*E*:*Z* #) | $PSS_{525}$ (*E*:*Z* #) |
|---|---|---|---|---|---|---|
| **1** | 380 nm | 394 nm | 6 min | 3 sec | <43:>57[a] | <84:>16[a] |
| **2** | 367 nm | 378 nm | 57 min | 3 min | 57:43[b] | 70:30[b] |

# $CH_3CN$, $ Aqueous, [a] Absorbance, [b] NMR

**Fig. 2** Simplified synthetic scheme (a), single-crystal X-ray structures (b), absorption spectra in acetonitrile at 25 °C before irradiation (BI, black lines) and at the PSS of 405 nm-wavelength irradiation ($405_{PSS}$, red lines) and at the PSS of 525 nm ($525_{PSS}$, blue lines) (absorbance changes for repeated $405_{PSS}$ and $525_{PSS}$ are shown in insets) (c and d) and photophysical parameters (e) of photoswitchable Wnt agonists **1** and **2**.

(>57% *cis*) as calculated from the absorption spectra (Fig. 2c, red curve). Compound **1** can also isomerize upon its exposure to 450 nm-wavelength irradiation (>24% *cis* at $PSS_{450\ nm}$) (Fig. S20†). $PSS_{525\ nm}$, achieved with light illumination at 525 nm, exhibited a *trans*-rich state, specifically >84% *trans* (Fig. 2c, blue curve). Similarly, compound **2** isomerized upon being irradiated with 405 nm-wavelength light, with a 43% *cis* isomer composition at $PSS_{405\ nm}$, and 70% *trans* isomer composition at $PSS_{525\ nm}$ as measured from the NMR spectra (Fig. 2c and S5†).

The half-life of the *cis* isomer of **1** in acetonitrile at 25 °C was found to be 6.4 min (Fig. S14†). In aqueous medium at 37 °C, the half-life was 3 seconds (Fig. S19†). Compound **2** showed a longer lifetime of the *cis* isomer, both in acetonitrile (57 min at 25 °C) and in aqueous medium (3 min at 37 °C), than did **1** (Fig. 2e, S23 and S27†). The electron-donation effect of the methylenedioxy group in **1** apparently caused the red-shifted absorption and shorter thermal stability of the *cis* isomer, as seen in other azobenzene derivatives.[27]

For a biological application, the photoswitch should be stable for 24 h in a reductive environment such as the cell cytoplasm. The potential ability of reductants like glutathione (GSH) to reduce the azo group (–N=N–) to the corresponding hydrazine (–NH–NH–) derivative can misestimate the actual potency of each isomer. We tested the stability levels of **1** and **2** by incubating them separately in a mixture of buffer and acetonitrile (50/50 v/v) glutathione (2 mM) reductant. Their absorbance spectra were then acquired, each before and after light irradiation (405 nm, 2 h for **2** and 450 nm, 12 h for **1**). The absorbance originating from the azo chromophore remained unchanged, indicating the excellent stability levels of the *trans* and *cis* isomers of **1** and **2** toward glutathione reductant (Fig. S30 and S31†). However, we found an unexpected photodegradation of **1** under continuous light irradiation in the presence or absence of glutathione (405 nm, 24 h or 450 nm, 24–72 h maintaining compounds in *cis* form ), as indicated by absorption spectra and NMR changes (Fig. S32–S36†). Such photodegradation was not observed for compound **2**.

## Biological studies

We then conducted the Wnt signaling activation experiment with photoswitchable agonists **1** and **2**. Due to the Wnt signaling pathway being directly connected to downstream gene expression, we performed a luminescence-based cellular assay in which the cells were transfected with a luciferase reporter gene (Luc gene). In general, Wnt signaling activation by an agonist leads to luciferase gene expression, which can be measured as luminescence output using a commercial luciferin substrate (Fig. 3a). In the current work, such an experiment was conducted for samples in a 24-well culture plate (293T cells) containing DMSO (negative control), **BML-284** (positive control) or photoswitchable agonists in the dark or under 405 nm-wavelength irradiation (0.05 mW $cm^{-2}$, 24 h at 37 °C and 5% $CO_2$). As expected, **BML-284** (5 μM) showed similar relative luminescences in the dark and in the presence of light irradiation (Fig. 3d light orange and orange bars). Interestingly, the photoswitchable agonists showed a clear difference in relative luminescence between the dark and light conditions in a dose-dependent manner (50–200 μM) (Fig. 3b–

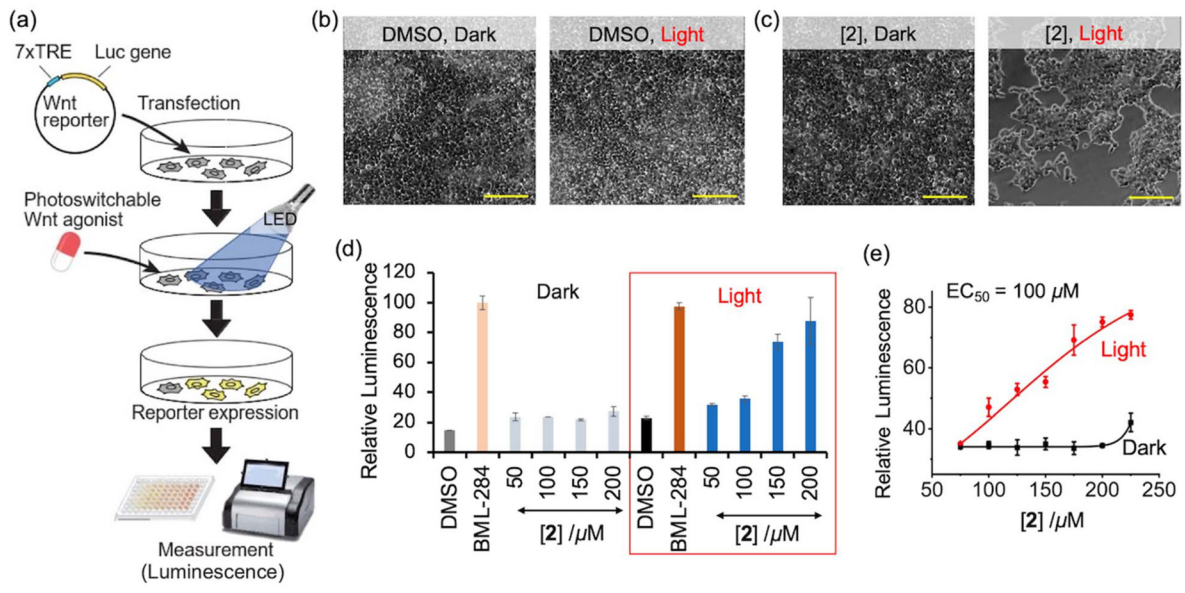


**Fig. 3** Schematic diagram showing a simplified workflow of the luminescence-based cellular assay, with 7xTRE as the plasmid used for the response element and the Luc gene as the plasmid for the luciferase-expressing gene (a). Microscopy images of 293T cells after 24 h of incubation of the cells in culture medium containing DMSO (0.4%) or 2 in the dark or light (405 nm, 0.05 mW $cm^{-2}$, 24 h) (scale bar 500 μm) (b and c). Bar graphs (d) non-linear fitting curves (e) of the relative luminescence, measured after treatment with DMSO (0.4%), of the non-photoswitchable agonist **BML-284** (5 μM) and photoswitchable agonist 2 (50–250 μM) in the dark or light (405 nm, 0.05 mW $cm^{-2}$, 24 h) (d and e).

d for **2**; light blue and blue bars). These results indicated that the *cis*-rich state of **2** formed upon light irradiation behaved as an agonist for Wnt signaling, similar to the behavior shown by the non-photoswitchable agonist **BML-284**. In contrast, the *trans*-rich state of **2**, like the DMSO control, did not show agonist activity. The $EC_{50}$ value calculated for **2** in the presence of light was 100 μM (Fig. 3e). A similar trend in the Wnt agonist activity for the *cis*-rich state was also observed for **1** (Fig. S40†), but with an efficiency lower than that of **2**, possibly due to the photodegradation of **1** under long-duration light exposure. We observed nearly 100% cell viability in our biological experimental condition (405 nm, 0.05 mW $cm^{-2}$; 450 nm, 7.94 mW $cm^{-2}$) (Fig. S42 and S43†). We also noticed a change in shape of the 293T cells in microscopy images for the experimental sets containing **BML284**[28] and *cis*-rich state of **2** formed after light irradiation, but no change in shape for the DMSO control or the *trans*-rich state of **2** (Fig. 3c and S38†). We assumed that the observed change in cell shape originated from the activation of the Wnt signaling pathway.

To examine whether **2** specifically activates Wnt/β-catenin signaling, we used a dominant negative form of TCF4, denoted as DN-TCF4[29] and which lacks the β-catenin-binding N-terminus region but is still able to bind to the target DNAs—and hence is a potent inhibitor of formation of the endogenous β-catenin/TCF complex. In the current work, expression of DN-TCF4 significantly suppressed the basal and compound **2**-stimulated activity of the Wnt reporter. This result was clearly indicative of **2** increasing Wnt reporter activity *via* activation of the endogenous β-catenin/TCF complex and hence demonstrating the specific activation of canonical Wnt/β-catenin signaling by **2** (Fig. S41†).

We are convinced that the difference in activity as Wnt agonists between the trans and *cis* isomers arises from their molecular shapes. Specifically, only *cis*-**1** and *cis*-**2** can adopt an angled configuration resembling the bent structure of the parent Wnt agonist **BML-284**. However, it cannot be excluded that the observed effects may also result from differences in cellular uptake or permeability between the *cis* and *trans* isomers.

### Spatiotemporal regulation

To demonstrate the effectiveness of our photoswitchable Wnt agonist in achieving localized agonist activity at a specific region of interest, we created two regions in a single well (six-well culture plate, well diameter 3.4 cm) treated with compound **2**, and exposed one area to visible light irradiation (~0.05 mW $cm^{-2}$) from the bottom, but not the other area (covered with aluminium foil) (Fig. 4a). After 24 h, cells were carefully scraped from the irradiated and non-irradiated regions of the well plate followed by taking luminescence measurements from these two samples, respectively. As expected, for the cells treated solely with DMSO, those exposed to the 405 nm-wavelength light showed luminescence similar to that taken from the covered area. However, cells treated with compound **2** and exposed to the light exhibited about 3 times higher luminescence than did cells treated with compound **2** and taken from the covered area. These results indicated that

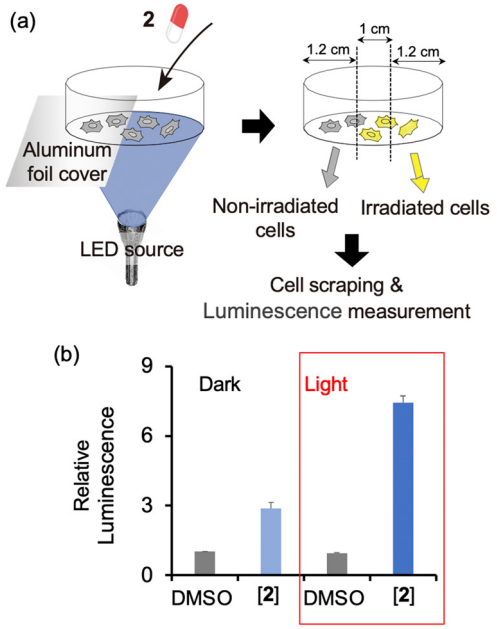


**Fig. 4** Schematic diagram showing a simplified workflow of selective activation of the Wnt signaling pathway; irradiated and non-irradiated cells at 1.2 cm from the sides of the well were scraped for luminescence measurements (a). Bar graph of relative luminescence intensity of cells treated with DMSO (0.4%) or photoswitchable agonist **2** (200 μM) in the dark or light (405 nm, 0.05 mW $cm^{-2}$, 24 h) (b).

the agonist activity of the Wnt signaling pathway by *cis* **2** was selectively activated only in the light-irradiated region with at least 10 mm spatial resolution (Fig. 4b).

## Conclusions

We developed novel photoswitchable agonists **1** and **2** that were found to enable photocontrol of the Wnt signaling pathway. The photoswitchable agonists each showed *trans* and *cis* isomers, which can be interconverted by visible light irradiation. Due to shape similarity with a known agonist **BML-284**, we found that only the *cis* isomer of the agonist activated the Wnt signaling pathway. We found higher agonist activity for Wnt signaling displayed by *cis*-**2** than by *cis*-**1**, due to an unexpected photodegradation of **1**. We also showed selective activation of the Wnt signaling pathway with a spatial resolution of 10 mm upon light irradiation of **2** in a model cell culture system. The visible-light–dependent control of Wnt signaling by these agonists may pave the way for the selective targeting of Wnt-sensitive cancer cells[30] and the spatiotemporal control of stem cell functions.[31]

## Experimental

### Synthesis

**Compound 1.** To a mixture of diamino methoxyphenyl pyrimidine (0.4 g, 1.1 eq.) and pyridine (2.4 mL) kept at 80 °C, a

nitroso derivative (0.4 g 1.0 eq.) was added. Then, to this mixture, 40% aqueous NaOH (100 μL) was added, and the resulting mixture was stirred at 80 °C for 1 h. Then, vacuum evaporation was carried out to remove the solvent, and the remaining material was subjected to column chromatography on silica using the EtOAc (30%)/hexane eluent to isolate pure compound (3% yield).

**Compound 2.** To a mixture of diamino methoxyphenyl pyrimidine (0.67 g, 1.1 eq.) and 1,4-dioxane (1 mL), nitrosobenzene (0.3 g, 1.0 eq.) was added. Then, to this mixture, 40% aqueous NaOH (5 mL) was added, and the resulting mixture was stirred at room temperature for 30 min. Then, vacuum evaporation was carried out to remove the solvent; water was added to the remaining material, and the resulting mixture was subjected to extraction with ethyl acetate and then dried with $MgSO_4$. Vacuum evaporation was carried out again to remove the solvent, and the remaining material was subjected to column chromatography on silica using the EtOAc (30%)/hexane eluent to isolate pure compound (8% yield).

### Measurement of thermal half-life

A freshly prepared solution of a tested sample was irradiated at 405 nm until it reached the photostationary state. It was then kept in the dark at 25 °C to achieve thermal isomerization back from *cis* to *trans*. Six to eight spectra were recorded at fixed time intervals, done under dark conditions to minimize the influence of the spectroscopy light beam on the thermal back isomerization. The first-order rate constant ($k$) for the thermal back isomerization reaction was then determined using the equation

$$\ln\frac{A_t}{A_0} = \ln\frac{\text{abs (BI)} - \text{abs (time)}}{\text{abs (BI)} - \text{abs (PSS)}} = -kt$$

where abs(BI) = absorbance at initial state at $\lambda_{max}$, abs(PSS) = absorbance at photostationary state at $\lambda_{max}$, and abs(time) = absorbance at $\lambda_{max}$ at a specified time interval for thermal back isomerization.

For a first order reaction, half-life ($t_{1/2}$) can be calculated using the equation

$$t_{1/2} = 0.693/k.$$

### Single-crystal X-ray crystallography

A small vial with 200 μL of a 10 mmol compound dissolved in chloroform was placed inside a larger container filled with 70 mL of hexane. The system was kept at −20 °C overnight, tightly sealed to prevent solvent evaporation. Over this period, the vapor concentration of hexane increased, gradually decreasing the solubility of the compound in chloroform and resulting in the slow precipitation of crystals from the solution.

### Cellular assay

HEK293T cells were obtained from American Type Culture Collection and maintained in DMEM supplemented with 10% FBS, 2 mM glutamine, and antibiotics (100 U $ml^{-1}$ of penicillin–streptomycin). Transfection of plasmids was performed with PEI Max transfection reagent (Polysciences) according to the manufacturer's protocol. For the measurement of beta-catenin/TCF transcriptional activity, 293T cells were transfected with the Wnt reporter (TOPFlash)[32] and the control reporter (pRL-TK) (Promega) plasmids, and cultured for 24 h. At 24 h after transfection, cells were treated with test compounds or DMSO and cultured for another 24 h with or without irradiation of the indicated wavelength of light. In each assay, the final concentration of DMSO was kept at 0.4% of the total aqueous medium. Firefly luciferase and Renilla luciferase activities in cell lysates were measured by using the Dual-Glo luciferase assay system in the GloMax Explorer system (Promega). We normalized the relative luciferase activity expressed from the Wnt reporter plasmid to the activity of Renilla luciferase expressed from the pRL-TK plasmid.

## Author contributions

S. A. conducted most of the experiments and data analysis. N. T. conceptualized the project and P. K. H. and N. M. C. helped with the synthesis and data analysis. M. I. helped with the cellular assay. K. T. and T. N. determined the X-ray crystal structure. N. T. supervised, and all authors contributed to writing the manuscript.

## Data availability

Data such as synthesis details and NMR, mass and absorption spectra are available in the ESI.†

## Conflicts of interest

"There are no conflicts to declare".

## Acknowledgements

S. A. and N. M. C. acknowledge Hokkaido University EXEX Doctoral Fellowship Program. P. K. H. acknowledges receipt of the 10th Hokkaido University Interdepartmental Symposium Research Grant Bronze Award. M. I. was supported by JSPS KAKENHI grant number 22K06874 and the Suhara memorial foundation.

## References

1 R. Hayat, M. Manzoor and A. Hussain, *Cell Biol. Int.*, 2022, **46**, 863–877.
2 Z. Steinhart and S. Angers, *Development*, 2018, **145**, dev146589.
3 X. Xu, M. Zhang, F. Xu and S. Jiang, *Mol. Cancer*, 2020, **19**, 165.

 

4 M. Haseeb, R. H. Pirzada, Q. U. Ain and S. Choi, *Cells*, 2019, **8**, 1380.
5 M. Kahn, *Nat. Rev. Drug Discovery*, 2014, **13**, 513–532.
6 J. L. Teo and M. Kahn, *Adv. Drug Delivery Rev.*, 2010, **62**, 1149–1155.
7 J. Liu, X. Wu, B. Mitchell, C. Kintner, S. Ding and P. G. Schultz, *Angew. Chem., Int. Ed.*, 2005, **44**, 1987–1990.
8 Z. Liu, P. Wang, E. A. Wold, Q. Song, C. Zhao, C. Wang and J. Zhou, *J. Med. Chem.*, 2021, **64**, 4257–4288.
9 M. Yu, K. Qin, J. Fan, G. Zhao, P. Zhao, W. Zeng, C. Chen, A. Wang, Y. Wang, J. Zhong, Y. Zhu, W. Wagstaff, R. C. Haydon, H. H. Luu, S. Ho, M. J. Lee, J. Strelzow, R. R. Reid and T. C. He, *Genes Dis.*, 2024, **11**, 101026.
10 V. V. Krishnamurthy, H. Hwang, J. Fu, J. Yang and K. Zhang, *J. Mol. Biol.*, 2021, **433**, 167050.
11 S. Lee, M. Cui, D. Lee, H. Kihoon, S. Woong and L. Dongmin, *iScience*, 2023, **26**, 106233.
12 I. M. Welleman, M. W. H. Hoorens, B. L. Feringa, H. H. Boersma and W. Szymański, *Chem. Sci.*, 2020, **11**, 11672–11691.
13 Q. Xu, C. Zhang, Z. Xu, L. Wang, Z. Liu, Z. Li and X. Shao, *J. Agric. Food Chem.*, 2023, **71**, 11048–11055.
14 Z. Li, Y. Wang, M. Li, H. Zhang, H. Guo, H. Ya and J. Yin, *Org. Biomol. Chem.*, 2018, **16**, 6988–6997.
15 M. P. O'Hagan, J. Ramos-Soriano, S. Haldar, S. Sheikh, J. C. Morales, A. J. Mulholland and M. C. Galan, *Chem. Commun.*, 2020, **56**, 5186–5189.
16 K. Hüll, J. Morstein and D. Trauner, *Chem. Rev.*, 2018, **118**, 10710–10747.
17 J. Volarić, W. Szymanski, N. A. Simeth and B. L. Feringa, *Chem. Soc. Rev.*, 2021, **50**, 12377–12449.
18 P. Kobauri, F. J. Dekker, W. Szymanski and B. L. Feringa, *Angew. Chem., Int. Ed.*, 2023, **62**, e202300681.
19 M. Banghart, K. Borges, E. Isacoff, D. Trauner and R. H. Kramer, *Nat. Neurosci.*, 2004, **7**, 1381–1386.
20 J. Levitz, C. Pantoja, B. Gaub, H. Janovjak, A. Reiner, A. Hoagland, D. Schoppik, B. Kane, P. Stawski, A. F. Schier, D. Trauner and E. Y. Isacoff, *Nat. Neurosci.*, 2013, **16**, 507–516.
21 N. Perur, M. Yahara, T. Kamei and N. Tamaoki, *Chem. Commun.*, 2013, **49**, 9935–9937.
22 N. N. Mafy, K. Matsuo, S. Hiruma, R. Uehara and N. Tamaoki, *J. Am. Chem. Soc.*, 2020, **142**, 1763–1767.
23 K. Matsuo, S. Thayyil, M. Kawaguchi, H. Nakagawa and N. Tamaoki, *Chem. Commun.*, 2021, **57**, 12500–12503.
24 S. Sahu, K. Yoshizawa, T. Yamamoto, R. Uehara and N. Tamaoki, *J. Am. Chem. Soc.*, 2024, **146**, 21203–21207.
25 J. A. Frank, M. Moroni, R. Moshourab, M. Sumser, G. R. Lewin and D. Trauner, *Nat. Commun.*, 2015, **6**, 7118.
26 J. Qi, A. S. Amrutha, S. Ishida-Ishihara, H. M. Dokainish, P. K. Hashim, R. Miyazaki, M. Tsuda, S. Tanaka and N. Tamaoki, *J. Am. Chem. Soc.*, 2024, **146**, 18002–18010.
27 M. Dong, A. Babalhavaeji, S. Samanta, A. A. Beharry and G. A. Woolley, *Acc. Chem. Res.*, 2015, **48**, 2662–2670.
28 Y. Zhang and F. Lu, *Scand. Cardiovasc. J.*, 2024, **58**, 2295785.
29 M. van de Wetering, E. Sancho, C. Verweij, W. de Lau, I. Oving, A. Hurlstone, K. van der Horn, E. Batlle, D. Coudreuse, A. P. Haramis, M. Tjon-Pon-Fong, P. Moerer, M. van den Born, G. Soete, S. Pals, M. Eilers, R. Medema and H. Clevers, *Cell*, 2002, **111**, 241–250.
30 A. Kazi, S. Xiang, H. Yang, D. Delitto, J. Trevino, R. H. Y. Jiang, M. Ayaz, H. R. Lawrence, P. Kennedy and S. M. Sebti, *Nat. Commun.*, 2018, **9**, 5154.
31 H. Clevers, K. M. Loh and R. Nusse, *Science*, 2014, **346**, 1248012.
32 P. J. Morin, A. B. Sparks, V. Korinek, N. Barker, H. Clevers, B. Vogelstein and K. W. Kinzler, *Science*, 1997, **275**, 1787–1790.